J Nanopart Res (2010) 12:2267–2276
DOI 10.1007/s11051-009-9795-7

RESEARCH PAPER

Room temperature growth of wafer-scale silicon nanowire arrays and their Raman characteristics

Dinesh Kumar · Sanjay K. Srivastava · P. K. Singh · K. N. Sood · V. N. Singh · Nita Dilawar · M. Husain

Received: 2 August 2009 / Accepted: 26 October 2009 / Published online: 8 November 2009
© Springer Science+Business Media B.V. 2009

Abstract We report a simple, inexpensive, and rapid process for large area growth of vertically aligned crystalline silicon nanowires (SiNWs) of diameter 40–200 nm and variable length directly on p-type (100) silicon substrate. The process is based on Ag-induced selective etching of silicon wafers wherein the growth of SiNWs was carried out using the aqueous HF solution containing Ag^{+} ions at room temperature in a Teflon vessel. Effect of etching time has been investigated to understand the evolution of SiNW arrays. It has been found that the length of SiNWs has a linear dependence on the etching time for small to moderate periods (0–2 h). However, etching rate decreases slowly for long etching times (>2 h). Scanning electron microscopy was used to study the morphology of the SiNW arrays. Structural and compositional analysis was carried out using Raman spectroscopy and high-resolution transmission electron microscopy equipped with energy dispersive X-ray spectroscopy. Orders of magnitude intensity enhancement along with a small downshift and broadening in the first-order Raman peak of SiNW arrays was observed in comparison to the bulk crystalline silicon.

Keywords Silicon nanowires · Electroless etching · Silver catalyst · Raman spectroscopy · High-rate synthesis

D. Kumar · S. K. Srivastava (✉) · P. K. Singh · K. N. Sood · N. Dilawar
National Physical Laboratory, Dr. K. S. Krishnan Marg, Pusa, New Delhi 110012, India
e-mail: srivassk@mail.nplindia.ernet.in

V. N. Singh
Department of Physics, Indian Institute of Technology, Hauz Khas, New Delhi 110016, India

M. Husain
Department of Physics, Faculty of Natural Sciences, Jamia Millia Islamia, New Delhi 110025, India

Introduction

In recent years, great efforts have been made to fabricate one-dimensional nanostructured materials for their novel size and dimensional-dependent physical and electronic properties (Rao et al. 2003; Xia et al. 2003). Silicon is the back bone of the microelectronics industry and therefore, silicon-based nanostructures such as silicon nanowires (SiNWs) have attracted special attention, and are, indeed, a potential candidate for applications in nanoscale optoelectronic devices (Huang et al. 2001; Huang et al. 2005; Koo et al. 2005). Several methods such as molecular beam epitaxy (Bauer et al. 2007), chemical vapor deposition (Meng et al. 2007; Latu et al. 2008), laser ablation (Yang et al. 2004), thermal evaporation (Pan et al. 2005), template assisted growth (Lew and Redwing 2003), oxide-assisted growth (Chuen et al. 2005), etc. have been successfully developed to

prepare one-dimensional silicon nanostructures. However, these growth processes generally need a high temperature, high vacuum, templates and special equipments, or hazardous silicon precursors which make them time consuming and expensive. A simple yet efficient way to fabricate large area, highly oriented, and length controllable SiNWs at low temperature is a challenge for the scientific community.

Several variant of catalytic wet chemical etching technique with Ag particles to prepare aligned SiNWs on silicon substrates close to room temperature ($\sim$50 °C) has been reported recently (Peng et al. 2003; Qiu et al. 2006; Fang et al. 2006). In one approach, cleaned silicon wafers are immersed in aqueous HF solution containing $AgNO_3$ (Peng et al. 2003; Qiu et al. 2006), while in another, Ag particles are first deposited either by a wet chemical process (electroless plating) or by a physical vapor deposition (thermal evaporation), and then immersed in chemical etching solution to grow SiNW arrays (Fang et al. 2006). Although both approaches are being used to make SiNWs, but the mechanism of formation of SiNWs during etching process, and role of Ag particles are still not clear, and is a subject of debate. One school of thought believes that Ag particles protect the silicon underneath from chemical etching and etching occurs in the surrounding area resulting silver capped SiNWs (Peng et al. 2003; Qui et al. 2005; Qiu et al. 2006), while other supports that the Ag particles only catalyze the etching of the silicon surface that is directly in contact with them (Fang et al. 2006). Hence, the two mechanisms are completely different and in some sense contradictory to each other. Most of these methods employ a Teflon vessel and, generally, the etching process is carried out under a sealed condition where the pressure is expected to be high, and therefore real growth conditions are not well-identified. Hence, there is need for a simpler process or modification in the existing processes. The objectives of the present study are: (i) to present a relatively simpler and controlled chemical etching process for large area aligned SiNWs growth, (ii) to study the growth mechanism and exact role of Ag in SiNWs growth, and (iii) to investigate Raman characteristics of SiNWs arrays, an area not very well-reported on SiNWs arrays prepared by wet chemical etching.

In this article, we present a relatively simple yet rapid method of fabricating large area (>5 cm diameter) SiNW arrays at room temperature on p-Si (100) substrates by Ag-induced wet chemical etching of silicon wafers in an aqueous HF solution containing silver nitrate ($AgNO_3$) in ambient conditions. The process is based on the mechanism of electroless metal deposition (EMD). The EMD process in an ionic metal-containing HF solution is based on micro electrochemical redox reaction, in which both cathodic and anodic reactions occur simultaneously at the metal/semiconductor interface (Gorostizee et al. 2000) which is an inexpensive technique, and has been widely used in microelectronics and metal coating applications (Wolfe et al. 2002). We have investigated the effect of etching time on the SiNW arrays length to understand the growth mechanism and the role of Ag particles. Systematic SEM investigations have suggested that formation of SiNWs was actually due to Ag-induced localized etching of silicon surface directly in contact with Ag particles, but not due to etching of Ag free surfaces. It was found that SiNWs always grow perpendicular to the silicon surface irrespective of positioning of the sample (vertical or horizontal) and the gravitational force. Raman characteristics of the SiNW arrays have also been investigated and compared with that of the bulk silicon substrate.

Experimental section

Growth of aligned SiNW arrays was carried out on p-type, B-doped (100) silicon (1–3 Ω cm) wafers in a Teflon beaker containing 5.0 mol L^{-1} aqueous HF solution and 0.02 mol L^{-1} $AgNO_3$ at room temperature ($\sim$25 °C) for different reaction times. Prior to the etching, the wafers were sequentially cleaned with acetone, ethanol, de-ionized water, and boiling in piranha solution (H_2SO_4:H_2O_2 = 3:1 by volume, for 60 min). Then, the wafers were rinsed thoroughly with de-ionized water followed by dipping in 10% HF solution to remove any surface oxides. The cleaned silicon wafers were then immersed in the etching solution. The etching time was varied keeping all other parameters, such as etching solution concentration, volume, temperature, etc., constant. The etched samples were found to be covered with thick Ag layer. The Ag layer was removed by conventional Ag etchants

consisting of $NH_3OH:H_2O_2 = 3:1$ solution. Finally, the as-prepared (wrapped with Ag layer) and the Ag removed samples were rinsed with de-ionized water, blown dry in nitrogen and subjected to further investigations. Morphology of the samples was examined by scanning electron microscope (SEM; LEO 440VP). The structure and chemical composition of the samples were investigated by high-resolution transmission electron microscope (HRTEM; FEI, Technai G20-stwin, 200K) equipped with energy dispersive X-ray spectrometer (EDS) (EDAX company, USA). Raman spectroscopy measurements were carried out using micro-Raman spectrometer at room temperature using an Ar ion laser of wavelength 514.5 nm (Model Innova 70, Coherent) as the excitation source. The Raman signals were measured in a back scattering geometry with a spectral resolution of 0.2 cm^{-1}. The scattered light was directed to the entrance slit of single stage Jobin-Yvon-Spex monochromator through a flexible optical fiber coupling. The Raman signal was detected using a water cooled Hamamatsu, (R943 PMT) photomultiplier tube which was connected at the output port of the monochromator.

Results and discussion

After electrochemical reactions, the silicon wafers were found wrapped with a thick gray color film. Typical cross-sectional and planer view SEM images of the as-prepared samples are shown in Fig. 1a and b. It can be clearly seen that the top thick film is composed of high density of treelike dendritic structures. Under thick film, vertically aligned SiNWs can be seen (Fig. 1b). The EDS analysis (as shown in Fig. 1a inset) revealed that thick film of dendrites was of pure Ag. The Ag dendrites were removed completely by treating the samples in NH_3OH and H_2O_2 mixture. A magnified top view of SiNWs array is shown in Fig. 1c and typical cross-sectional view of the vertically aligned SiNW arrays formed on Si wafers after removal of Ag layer is shown in Fig. 1d, which are bundled together (after treating in Ag

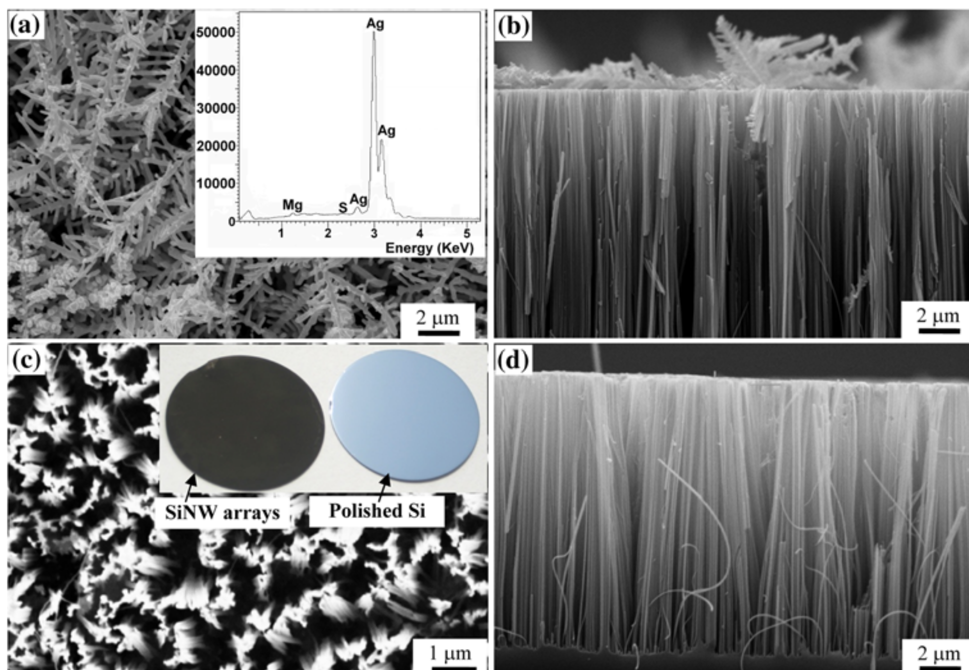

Fig. 1 SEM images showing (**a**) planar top view, (**b**) Cross-sectional view of the as prepared SiNW samples covered with thick dendritic film. Inset of (**a**) shows corresponding EDS spectrum confirming dendritic structures of Ag. (**c**) Planar top view and (**d**) cross-sectional view of the SiNW arrays after removal of Ag dendrites. Inset of (**c**) shows the optical images of a polished Si wafer and wafer with SiNWs arrays

etchant solution, cleaning with DI water followed by drying), and are firmly attached with the substrate. It is interesting to see that the silicon sample with SiNW arrays surface look black in color after Ag removal as shown by optical photograph in the inset of Fig. 1c along with a polished wafer for comparison. The black surface is due to extremely low reflectivity and hence, may be a potential candidate for an effective antireflective layer in silicon-solar cells (Koynov et al. 2006; Yoo et al. 2006).

Figure 2a shows the representative bright-field TEM image of the as-grown SiNWs. The lateral width of SiNWs was estimated to be in the range of 40–200 nm. The corresponding selected area electron diffraction (SAED) pattern with the electron beam parallel to the [*100*] zone axis is shown in the inset (a) indicating crystalline nature of the nanowires. Figure 2b shows the HRTEM image of a section of the nanowire (shown in Fig. 2a). The inter-planar spacing is estimated to be ~0.31 nm corresponding to (*111*) planes of silicon. The SAED and HRTEM analyses confirmed that the SiNWs were single crystalline in nature with axial orientation along [*100*] direction, which is identical to the orientation of the wafer used. The representative EDS spectrum of the SiNW is shown in Fig. 2c. The strongest signal observed corresponds to Si reconfirming that nanowires are made purely of silicon and no traces of metallic impurities such as Ag was observed. The signal corresponding to Cu and C are attributed to carbon-coated Cu microgrids used for TEM specimen preparation.

We performed time-dependent etching of wafers to investigate the SiNWs growth rate and mechanism associated with it. Figure 3 shows the variation of SiNW arrays length with etching time. It was found that the SiNWs length increased linearly with etching time up to 2 h when the length of nanowires is ~30 μm. Thereafter, the SiNW arrays growth rate slows down as can be seen from the deviation of the wire length from the linearity. The expanded plot of the linear dependence of SiNWs length versus etching time is shown in the inset of the Fig. 3. It is believed that decrease of SiNW growth rate (etching rate) could be due to continuously decreasing Ag^+ content in a given etching solution because Ag^+ get reduced to Ag to form a thick Ag film over the wafer during etching. The thick Ag film deposited around the

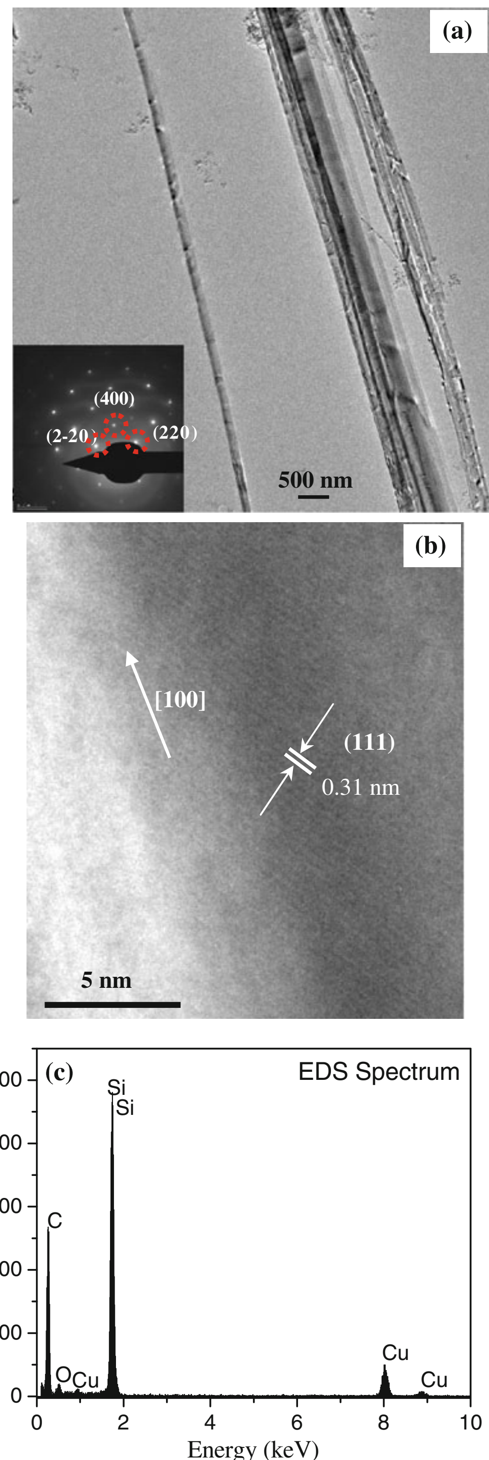

Fig. 2 **a** Bright field TEM image of Si nanowires, corresponding SAED pattern is shown in the inset, **b** HRTEM image of a nanowire showing single crystalline, and **c** representative EDS spectrum of a single nanowire

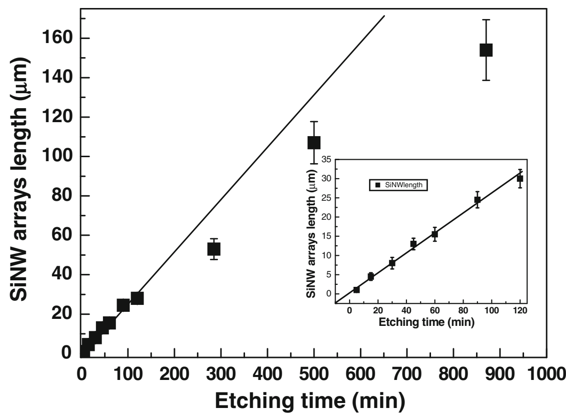

Fig. 3 SiNW arrays length versus etching time plot for Si [*100*] wafers at 25 °C etching temperature. Inset shows the expanded view of the plot for 0–2 h etching time

substrate may also slow down the etching rate of silicon underneath this film. Further, HF reactivity, which is exposed to the ambience, may also be affected after long process time. The average etching rate was estimated to be $\sim$180 nm min^{-1} for an etching time of 15 h and $\sim$250 nm min^{-1} in the linear range (0–2 h). The curve clearly indicates that the SiNW arrays of desired length could be obtained at room temperature by judicially controlling the etching time. Figure 4a–d shows the cross-sectional SEM images of SiNW arrays produced at room temperature ($\sim$25 °C) for 5, 15, 45, and 90 min, respectively. It is evident from the SEM images that SiNWs are tangled with each other after a certain length and held together in bundles which could be due to surface tensional forces which are effective during drying process. Subsequently the van der Waal forces hold SiNWs together. At times, SiNWs collapse as their length become too long. It is also observed that the SiNWs have uniform thickness (or diameter) throughout the length whether grown for short or long time periods.

Catalytic activity of Ag nanoparticles is well-known in electrochemical etching of silicon in HF solution where deep cylindrical nano holes were produced in [*100*] silicon using Ag nanoparticles as catalyst (Tsujino and Matsumura 2005). The process is called as metal-assisted chemical etching of silicon (Li and Bohn 2000). The mechanism of formation of vertically aligned SiNW arrays can be understood as being a self-assembled Ag-induced selective etching process based on localized microscopic electrochemical cell model as presented schematically in Fig. 5. The process is based on the continuous galvanic displacement of Si by Ag^+ via $Ag^+ \rightarrow Ag$ reduction on the silicon surface and hence forming many local nano-electrochemical cells on the silicon surface. The deposited Ag nanoparticles act as active cathode and silicon surface in contact with the Ag nanoparticles as active anode. In brief, Ag^+ ions get reduced to Ag onto the silicon surface by injecting holes into the Si valence band and oxidizing the silicon surface locally

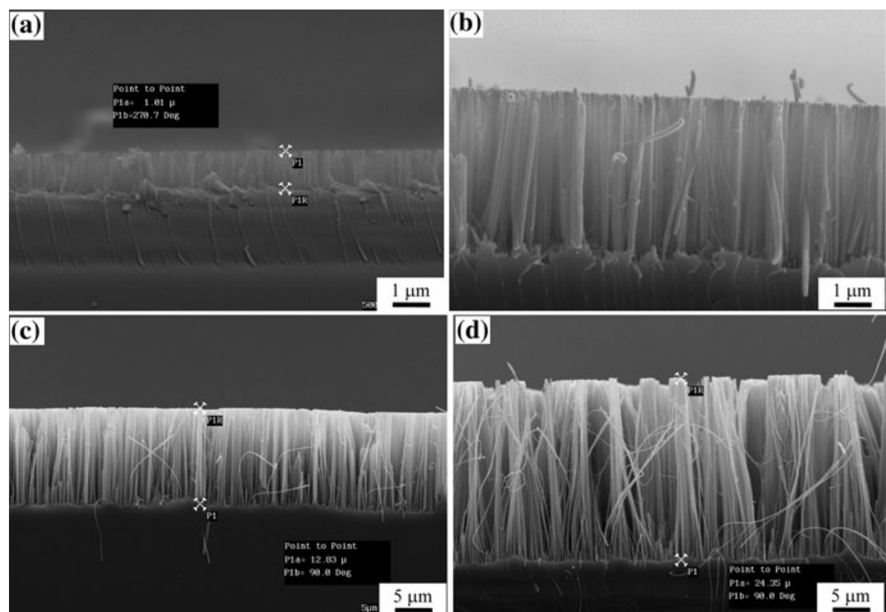

Fig. 4 Cross-sectional SEM images of SiNW arrays produced at room temperature ($\sim$25 °C) for (**a**) 5 min, (**b**) 15 min, (**c**) 45 min, and (**d**) 90 min

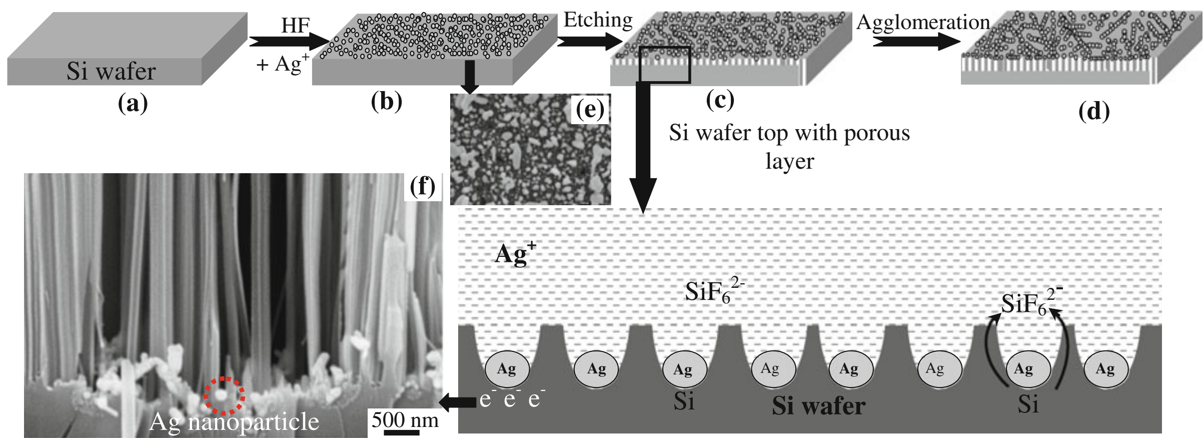

Fig. 5 Schematics of the SiNWs growth mechanism by Ag-induced selective chemical etching of silicon surface in HF–$AgNO_3$ solution via self-assembled nano-electrochemical cell model

in contact with Ag. The oxidized surface is subsequently etched away by HF. The initial reduction of Ag^+ results Ag nanoclusters as observed clearly by SEM image in Fig. 6a after 30 s of etching process which probably restricts the oxidation of silicon surface and etching process occurs locally. The deposited Ag nanoclusters are initially uniformly distributed throughout the surface of the silicon wafer (as shown schematically in Fig. 5b and SEM image in Fig. 6a). Further reduction of Ag^+ occurs on the Ag nanoclusters being an active cathode by electron transfer from the underlying wafer (Ag being relatively highly electronegative than the silicon and hence provide easy injection path for holes), but does not occur on the uncovered Si surface. The increasing size of the Ag clusters via this mechanism is shown schematically in Fig. 5c and d, and is confirmed by the SEM images in Fig. 6a–c for etching times of 30, 60, and 120 s, respectively. It is to be noticed here that density of Ag nanoclusters on the surface decreases with etching time as can be seen from the SEM images shown in Fig. 6a and b of the samples etched for 30 and 60 s. This may be attributed to the trapping of Ag clusters followed by their downward movement in the forming pores. Closer examination of SEM image (Fig. 5f) shows presence of Ag particles (confirmed by EDS study, not shown here) of different sizes lying in the pores at the bottom of the SiNW arrays. This, indeed, is a clinching evidence of Ag nanoparticle-induced electrochemical etching of silicon surfaces which is in direct contact with the Ag particles, and hence this process is completely different from the mechanisms proposed earlier (Peng et al. 2003; Qui et al. 2005, 2006). However, it favors the observation by Fang et al. (2006). The complete self-assembled Ag-induced redox reaction is presented schematically in magnified view of Fig. 5c. In the next step, Ag nanoclusters agglomerate to form the dendritic structures and hence a non-compact Ag film (as shown in Fig. 5d). The self-assembly of Ag nanoclusters to the dendritic structure and lack of compact Ag film formation lead to selective oxidation and dissolution of Si in the aqueous HF–$AgNO_3$ solution. The dimensions of the nanowires are primarily controlled by these Ag nanoclusters and their network after they get trapped into the silicon. Figure 6d–f shows the SEM images of the silicon surface after removal of Ag nanoclusters completely from the samples corresponding to the samples shown in Fig. 6a–c, respectively. Here, we can see that the pits size over Si surface increases initially as dimensions of Ag nanoclusters increases and results into a porous structure (see Fig. 6d–f). Once the Ag nanoclusters get trapped into the silicon pores, they move deeper and deeper resulting into the 1-D nanostructures or SiNWs.

Figure 6g shows the SEM image of a silicon wafer, in which SiNW arrays can be seen over the top, as well as bottom surface. Such type of growth was observed when etching solution finds its way to the back surface of the wafer (i.e., SiNWs growth against the gravity) and therefore, this observation completely rules out the role of gravitational effect. It is believed that localized electrostatic force (between

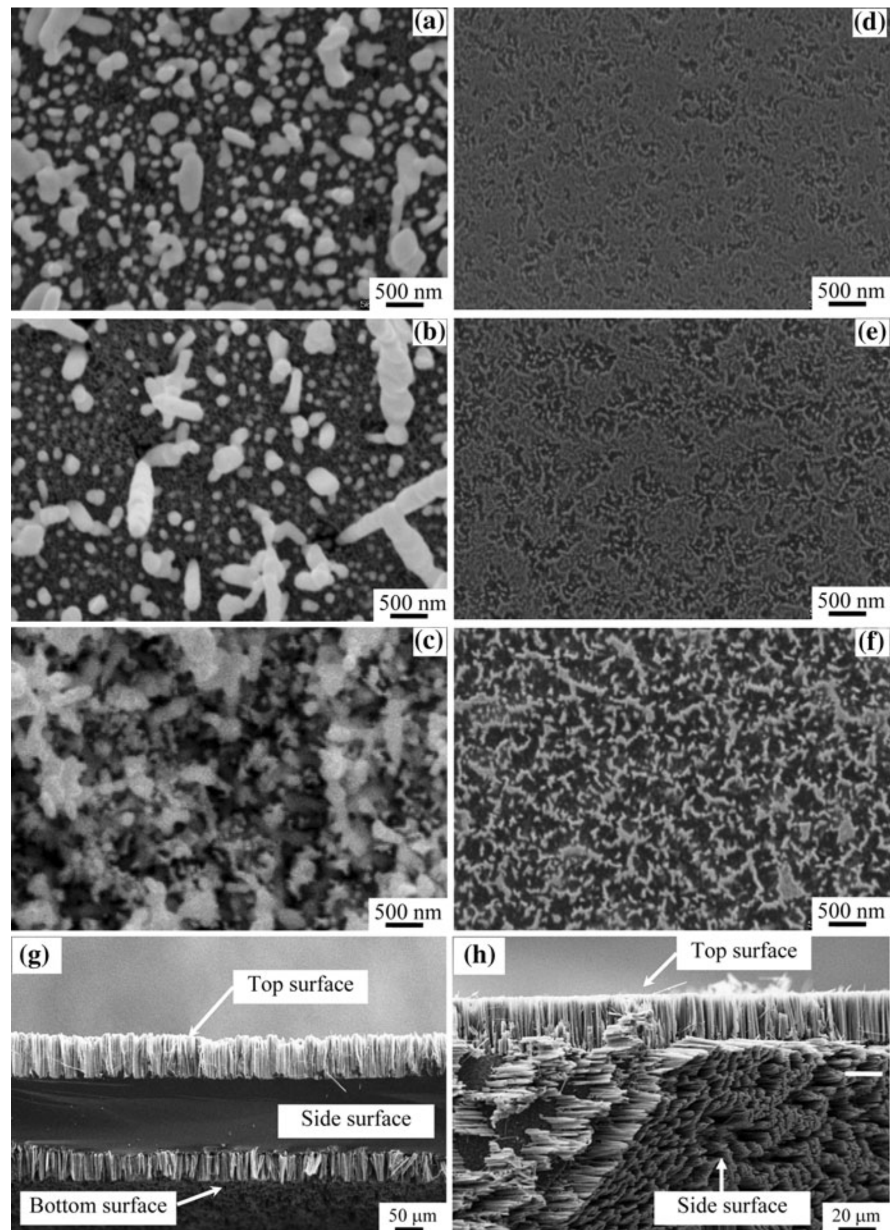

Fig. 6 Typical top view shown in **a**, **b**, and **c** of the initial phase of SiNWs growth for 30, 60, and 120 s, respectively, while **d**, **e**, and **f** shows the corresponding top view after Ag removal. Typical cross-sectional SEM images showing growth of SiNWs oriented perpendicular to (**g**) both top and bottom surfaces and (**h**) side surface of the silicon wafers indicating etching of silicon surface always occurs normal to the surface irrespective of the positioning of silicon wafers in the etching solution

negatively charged Ag particles in contact with silicon surface and positively charged silicon surface underneath Ag particles or localized nano-sized cathodes and anodes) may be the driving force for directional movement of Ag nanoparticles in the pores and being in contact with silicon surface irrespective of surface positioning of silicon substrates. This assumption is further supported from Fig. 6h, where the SiNWs growth from the sides (i.e., edges) of the silicon wafer along with the top surface is shown. This can happen only when the movement of Ag nanoparticles is in horizontal direction without being affected by gravitational force. Therefore, it can be concluded that SiNWs growth takes place normal to the surface, and is independent of the positioning of the samples surface. However, the present study is limited to [*100*] silicon only.

From the present study, we speculate that orientation-dependent electrochemical properties of silicon in HF solution may play a decisive role in the growth

of directional nanowires. It is known that silicon dissolves easily from the [*100*] face in a fluoride containing solution, therefore, pores are preferentially formed in the [*100*] direction (Lehman 1993). However, once the etching starts in the [*100*] direction the pores are expected to grow in this direction due to larger contact area compared to the other directions (Tsujino and Matsumura 2007) resulting in nanowires with [*100*] axial orientation. However, to establish this, further investigations are needed.

Raman spectroscopy

The comparative Raman spectra of bulk single crystal silicon substrate (used for SiNW arrays preparation) and the substrate with SiNW arrays are shown in Fig. 7. A Raman peak at 524.5 cm^{-1} with the full width at half maximum (FWHM) of 9.2 cm^{-1} is observed in the case of silicon substrate without SiNW arrays which can be attributed to scattering of the first-order optical phonon of crystalline silicon (Li et al. 1999). In comparison, the first order Raman peak of SiNW arrays is observed at 522 cm^{-1} with a FWHM of 14.8 cm^{-1} (a downshift of $\sim$2.5 cm^{-1}). The peak is broadened and little asymmetric toward lower wave numbers. Further, the first-order Raman intensity was enhanced by an order of magnitude compared to that of bulk silicon as shown in Fig. 7. Two effects that could lead to the enhancement of

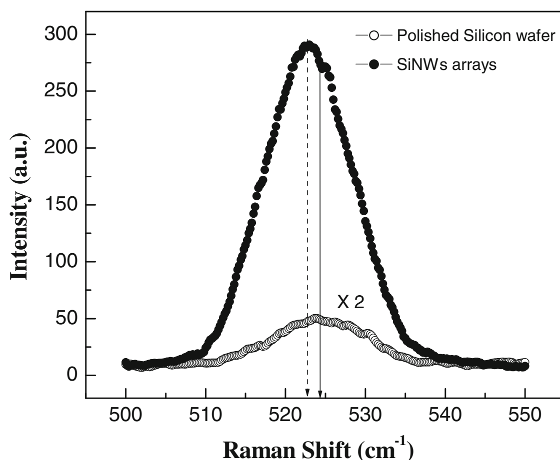

Fig. 7 Raman spectra of SiNWs arrays and bulk crystalline polished silicon substrate showing about an order of magnitude enhancement of Raman intensity for SiNWs along with broadening and peak shift to lower wave number

Raman intensity may be (i) the transmitted excitation intensity into the material should increase due to decreased area fraction of silicon after etching, leading to minimization of losses due to diffuse scattering, and (ii) the Raman back scatter traveling toward the surface may have encountered the nano-interstice surface between the SiNWs causing enhancement factor for the light excitation (Tian et al. 2005). The dark black appearance of SiNW arrays surface also indicate the minimization of reflectance and hence scattering losses. It may be attributed to network of SiNWs, which cause multiple reflection of excitation intensity eventually leading to maximum absorption. In contrast to earlier report (Li et al. 2005), significant downshift and asymmetric broadening of line width is not observed in the present case. It has been established that peak shifting and asymmetric broadening of the peak in low dimensional materials, such as nanowires, nanorods, nanodots, etc. occurs due to finite size and hence phonon quantum confinement effect causing relaxation of Raman selection rule $q \neq 0$ and allow participation of phonons away from the Brillouin-zone center (Γ point); and that the quantum confinement effect is observable effectively only for structures with at least one of the three main dimensions are smaller than $\sim$15 nm (Piscanec et al. 2003). However, SiNWs formed in the present study were large in diameter (40–200 nm) and length (tens of microns) and this may be a reason of non-appearance of significant downshift. A small downshift and asymmetric broadening of the silicon Raman peak (at $\sim$520 cm^{-1}) in the case of silicon nanowires also occurs due to local heating by laser which is, generally, not observed in bulk silicon (Piscanec et al. 2003).

Conclusions

We have demonstrated a relatively simple, cheap, and rapid (growth rate $\sim$180 nm min^{-1}) room temperature process for wafer-scale growth of vertically aligned SiNW arrays of controlled length on p-type [*100*] silicon substrates using electroless wet chemical etching of Si in aqueous HF–$AgNO_3$ solution. Structural analyses of the as grown SiNWs revealed that Si nanowires were single crystalline having axial orientation identical to the silicon wafer used. SiNWs are formed due to the selective etching of the silicon

surface directly in contact with Ag nanoclusters via self-assembled nano-electrochemical process wherein the Ag nanoclusters which are formed due to the reduction of Ag^{+} over the silicon surface acts as the catalyst during etching process. The growth of SiNW arrays takes place normal to the silicon surface governed by the localized electrostatic force between nanosized cathodes and anodes. The length of the SiNWs was found to be linearly dependent on etching time at room temperature for $\sim$2 h of etching and after that non-linearity set in. However, the SiNW as long as 150 μm could be made after 15 h of processing. Increased first-order Raman peak intensity (by an order of magnitude) was observed in SiNW arrays compared to that of bulk silicon substrates. Furthermore, the present investigations helped in resolving the paradox on the role of Ag in SiNW arrays formation by the wet chemical process. The simplicity of the present process may lead to the advancements and applications of SiNWs in opto-electronics and nano-electronic devices as well as for silicon-solar cells.

Acknowledgments The present study is funded by the Council of Scientific and Industrial Research (CSIR) India under network project SIP-017. One of the authors, Dinesh Kumar, is grateful to University Grant Commission (UGC), India for providing financial support in the form of research fellowship during this study.

References

Bauer J, Fleischer F, Breitenstein O, Schubert L, Werner P, Gosele V, Zacharias M (2007) Electrical properties of nominally undoped silicon nanowires grown by molecular-beam epitaxy. Appl Phys Lett 90:012105(1)–012 105(3)

Chuen YL, Chou LJ, Cheng SL, He JH, Wu WW, Chen LJ (2005) Synthesis of taperlike Si nanowires with strong field emission. Appl Phys Lett 86:133112(1)–133112(3)

Fang H, Wu Y, Zhao J, Zhu J (2006) Silver catalysis in the fabrication of silicon nanowire arrays. Nanotechnology 17: 3768–3774

Gorostizee P, Kulandainathan MA, Diaz R, Sanz F, Allongue P, Morante JR (2000) Charge exchange processes during the open-circuit deposition of nickel on silicon from fluoride solutions. J Electrochem Soc 147:1026–1030

Huang Y, Duan X, Cui Y, Lauhon LJ, Kim K, Lieber CM (2001) Logic gates and computation from assembled nanowire building blocks. Science 294:1313–1317

Huang Y, Duan XF, Lieber CM (2005) Nanowires for integrated multicolor nanophotonics. Small 1:142–147

Koo S, Li Q, Edelstein MD, Richter CA, Vogel EM (2005) Enhanced channel modulation in dual-gated silicon nanowire transistors. Nano Lett 5:2519–2523

Koynov S, Brandt MS, Stutzmann M (2006) Black nonreflecting silicon surfaces for solar cells. Appl Phys Lett 88: 203107(1)–203107(3)

Latu RL, Mouchet C, Cayron C, Rouviere E, Simonato JP (2008) Growth parameters and shape specific synthesis of silicon nanowires by the VLS method. J Nanopart Res 10: 1287–1291

Lehman V (1993) The physics of macropore formation in low doped n-type silicon. J Electrochem Soc 140:2836–2843

Lew KK, Redwing JM (2003) Growth characteristics of silicon nanowires synthesized by vapor–liquid–solid growth in nanoporous alumina templates. J Cryst Growth 254:14–22

Li X, Bohn PW (2000) Metal-assisted chemical etching in HF/H_2O_2 produces porous silicon. Appl Phys Lett 77:2572–2574

Li BB, Ju DP, Zhang SL (1999) Raman spectral study of silicon nanowires. Phys Rev B 59:1645–1648

Li C, Fang G, Sheng S, Chen Z, Wang J, Ma S, Zhao X (2005) Raman spectroscopy and field emission properties of aligned silicon nanowire arrays. Physica E 30:169–173

Meng C-Y, Shih B-L, Lee S-C (2007) Silicon nanowires synthesized by vapor–liquid–solid growth on excimer laser annealed thin gold film. J Nanopart Res 9:657–660

Pan H, Lim S, Poh C, Sun H, Wu X, Feng Y, Lin J (2005) Growth of Si nanowires by thermal evaporation. Nanotechnology 16:417–421

Peng KQ, Yan YJ, Gao SP, Zhu J (2003) Dendrite assisted growth of silicon nanowires in electroless metal deposition. Adv Funct Mater 13:127–132

Piscanec S, Contoro M, Ferrari AC, Zapien JA, Lifshitz Y, Lee ST, Hoffman SH, Robertson J (2003) Raman spectroscopy of silicon nanowires. Phys Rev B 68:241312(1)–2413 12(4)

Qiu T, Wu XL, Siu GG, Chu PK (2006) Intergrowth growth mechanism of silicon nanowires and silver dendrites. J Electron Mater 35:1879–1884

Qui T, Wu XL, Mei YF, Wan GJ, Chu PK, Siu GG (2005) From Si nanotubes to nanowires: synthesis, characterization, and self-assembly. J Cryst Growth 277:143–148

Rao CNR, Deepak FL, Gundiah G, Govindraj A (2003) Inorganic nanowires. Prog Solid State Chem 31:5–147

Tian L, Ram KB, Ahmad I, Menon L, Holtz M (2005) Optical properties of Si nanopore arrays. J Appl Phys 97:026101 (1)–026101(3)

Tsujino K, Matsumura M (2005) Boring deep cylindrical nanoholes in silicon using silver nanoparticles as a catalyst. Adv Mater 17:1045–1047

Tsujino K, Matsumura M (2007) Morphology of nanoholes formed in silicon by wet etching in solutions containing HF and H_2O_2 at different concentrations using silver nanoparticles as catalysts. Electrochem Acta 53:28–34

Wolfe DB, Love JC, Paul KE, Chabinye ML, Whitesides GM (2002) Fabrication of palladium-based microelectronic devices by microcontact printing. Appl Phys Lett 80:2222–2224

Xia Y, Yang P, Sun Y, Wu Y, Mayers B, Gates B, Yin Y, Kim F, Yan H (2003) One-dimensional nanostructures:

synthesis, characterization, and applications. Adv Mater 15:353–389

Yang YH, Wu SJ, Chiu SH, Lin P, Chen YT (2004) Catalytic growth of silicon nanowires assisted by laser ablation. J Phys Chem B 108:846–852

Yoo JS, Parm IO, Gangopadhyay U, Kim K, Dhungel SK, Mangalaraj D, Yi JS (2006) Black silicon layer formation for application in solar cells. Sol Energy Mater Sol Cells 90:3085–3093